NASA/TM—2002-211906/PART2

A Deterministic Interfacial Cyclic Oxidation Spalling Model: Part 2.—Algebraic Approximation, Descriptive Parameters, and Normalized Universal Curve

James L. Smialek
Glenn Research Center, Cleveland, Ohio

December 2002

The NASA STI Program Office . . . in Profile

Since its founding, NASA has been dedicated to the advancement of aeronautics and space science. The NASA Scientific and Technical Information (STI) Program Office plays a key part in helping NASA maintain this important role.

The NASA STI Program Office is operated by Langley Research Center, the Lead Center for NASA's scientific and technical information. The NASA STI Program Office provides access to the NASA STI Database, the largest collection of aeronautical and space science STI in the world. The Program Office is also NASA's institutional mechanism for disseminating the results of its research and development activities. These results are published by NASA in the NASA STI Report Series, which includes the following report types:

- TECHNICAL PUBLICATION. Reports of completed research or a major significant phase of research that present the results of NASA programs and include extensive data or theoretical analysis. Includes compilations of significant scientific and technical data and information deemed to be of continuing reference value. NASA's counterpart of peer-reviewed formal professional papers but has less stringent limitations on manuscript length and extent of graphic presentations.

- TECHNICAL MEMORANDUM. Scientific and technical findings that are preliminary or of specialized interest, e.g., quick release reports, working papers, and bibliographies that contain minimal annotation. Does not contain extensive analysis.

- CONTRACTOR REPORT. Scientific and technical findings by NASA-sponsored contractors and grantees.

- CONFERENCE PUBLICATION. Collected papers from scientific and technical conferences, symposia, seminars, or other meetings sponsored or cosponsored by NASA.

- SPECIAL PUBLICATION. Scientific, technical, or historical information from NASA programs, projects, and missions, often concerned with subjects having substantial public interest.

- TECHNICAL TRANSLATION. English-language translations of foreign scientific and technical material pertinent to NASA's mission.

Specialized services that complement the STI Program Office's diverse offerings include creating custom thesauri, building customized databases, organizing and publishing research results . . . even providing videos.

For more information about the NASA STI Program Office, see the following:

- Access the NASA STI Program Home Page at ***http://www.sti.nasa.gov***

- E-mail your question via the Internet to help@sti.nasa.gov

- Fax your question to the NASA Access Help Desk at 301–621–0134

- Telephone the NASA Access Help Desk at 301–621–0390

- Write to:
  NASA Access Help Desk
  NASA Center for AeroSpace Information
  7121 Standard Drive
  Hanover, MD 21076

NASA/TM—2002-211906/PART2

A Deterministic Interfacial Cyclic Oxidation Spalling Model: Part 2.—Algebraic Approximation, Descriptive Parameters, and Normalized Universal Curve

James L. Smialek
Glenn Research Center, Cleveland, Ohio

National Aeronautics and
Space Administration

Glenn Research Center

December 2002

Acknowledgments

The author is grateful for the mathematical analysis provided by Dr. Brian Good, NASA GRC, who provided a simplification of $\sum_{1}^{j}\sqrt{i}$, enabling the derivation of the descriptive parameters and the concept of a universal cyclic oxidation curve.

This report is a formal draft or working paper, intended to solicit comments and ideas from a technical peer group.

This report contains preliminary findings, subject to revision as analysis proceeds.

Available from

NASA Center for Aerospace Information
7121 Standard Drive
Hanover, MD 21076

National Technical Information Service
5285 Port Royal Road
Springfield, VA 22100

Available electronically at http://gltrs.grc.nasa.gov

A Deterministic Interfacial Cyclic Oxidation Spalling Model: Part 2.—Algebraic Approximation, Descriptive Parameters, and Normalized Universal Curve

James L. Smialek
National Aeronautics and Space Administration
Glenn Research Center
Cleveland, Ohio 44135

Abstract.—A cyclic oxidation interfacial spalling model has been developed in Part 1. The governing equations have been simplified here by substituting a new algebraic expression for the series $\Sigma\sqrt{i}$ (Good-Smialek approximation). This produced a direct relationship between cyclic oxidation weight change and model input parameters. It also allowed for the mathematical derivation of various descriptive parameters as a function of the inputs. It is shown that the maximum in weight change varies directly with the parabolic rate constant and cycle duration and inversely with the spall fraction, all to the ½ power. The number of cycles to reach maximum and zero weight change vary inversely with the spall fraction, and the ratio of these cycles is exactly 1:3 for most oxides. By suitably normalizing the weight change and cycle number, it is shown that all cyclic oxidation weight change model curves can be represented by one universal expression for a given oxide scale.

1. Introduction

In Part 1 a model has been developed to describe the iterative scale growth and spalling process that occurs during cyclic oxidation of high temperature materials [1]. Parabolic scale growth and interfacial spalling of a constant surface area fraction, in the thickest region of the scale, have been postulated. This ultimately results in a segmented scale morphology. Model inputs consist of the parabolic growth rate constant, k_p, cycle duration, Δt, the spall area fraction, F_A, (which is equal to the inverse of the number of oxide area segments, n_o, and oxide stoichiometry, S_c, (the ratio of oxide to oxygen weight in the scale).

The relationships for cyclic oxidation net weight change according to this deterministic, interfacial, cyclic oxidation spalling model (DICOSM, Part I) are as follows [1]:

For cycle number $j \leq n_o$ (Case A):

$$\left(\frac{\Delta W}{A}\right)_A = F_A\sqrt{k_p\Delta t}\left\{(2-S_c)\sum_{i=1}^{j}\sqrt{i}+(n_o-j-1)\sqrt{j}\right\} \qquad [1a]$$

And for cycle number $j \geq n_o$ (Case B):

$$\left(\frac{\Delta W}{A}\right)_B = F_A\sqrt{k_p\Delta t}\left\{(2-S_c)\sum_{i=1}^{n_o}\sqrt{i}+[(1-S_c)(j-n_o)-1]\sqrt{n_o}\right\} \qquad [1b]$$

where $\Delta W/A$ is the net sample specific weight (mass) change and j is the cycle number. A baseline case was presented for comparison in the sensitivity studies, where j, the number of cycles, was allowed to reach 2000, and n_o, the number of segments, was typically 1000, i.e., F_A=0.001, k_p=0.01 mg^2/cm^4h, Δt=1 h, and S_c=2.0. Other model outputs include the total amount (mass) of oxygen and metal consumed, the total amount of oxide spalled, and the mass fraction of oxide spalled. The outputs all follow typical well-behaved trends with the input variables.

This model produced all the characteristic features normally associated with cyclic oxidation weight change curves or models thereof: an initial maximum, followed by decreasing and eventually negative weight change, and finally a steady-state linear rate of weight loss (concurrent with attaining both a limiting oxide thickness and constant mass fraction of scale spalled each cycle).

These features all vary with the input parameters in a regular fashion, as have been demonstrated in previous modeling studies. Those efforts have resulted in reasonable descriptions of cyclic behavior as a function of the input parameters and allow one to see approximate functional interdependencies. However, any mathematical expression describing these dependencies has been indirect, i.e., by regression analysis of the results of many model cases [2] or by trial and error fits to various functions [3].

There would be value to describing these trends for the DICOSM model as well. Given its mathematical simplicity, there is greater potential for obtaining a more precise, direct relationship with the input parameters. The DICOSM calculations are only algebraic except for the factor $\Sigma\sqrt{i}$. This factor, requiring an iterative calculation, appears in all the model outputs. The full calculation thus precludes any elementary mathematical operations or descriptions of the outputs in simple algebraic terms. An algebraic solution to this factor would allow the model to be calculated directly without the need of a computer program. Furthermore, the mathematical relationships between the model input parameters and outputs would be more transparent.

Therefore, the purpose of this study in Part 2 is to simplify the basic model equations. Specifically, a substitution for the summation series is addressed, and the degree of error associated with this approximation is characterized. Using this substitution, simplified DICOSM equations are obtained. Characteristic parameters, describing the key elements of cyclic oxidation weight change behavior, are derived as a function of the input parameters. Finally, the concept of a universal cyclic oxidation curve is proposed, as enabled by these simplified relationships.

2. Results and Discussion

2.1 The Good-Smialek Approximation.

An attempt was made to find a mathematical expression for $\Sigma\sqrt{i}$ by Dr. Brian Good and the use of the math program, *Mathematica* © [4]. An expansion with the terms $j^{1/2}$, $j^{2/2}$ $j^{3/2}$, $j^{4/2}$, $j^{5/2}$ + K was found (G-A):

$$\sum_{1}^{j}\sqrt{i}_{GA} = aj^{1/2} + bj^{2/2} + cj^{3/2} + dj^{4/2} + ej^{5/2} + K \qquad [2]$$

where the coefficients produced by linear regression were identified as:

a	0.48957
b	0.0012181
c	0.66660
d	1.8489×10^{-6}
e	-1.90171×10^{-9}
K	–0.169614

This equation has yielded an extremely accurate expression for any j>10, with a maximum error of only 1.2 percent at j = 1. Since we are concerned with relatively large numbers of cycles, this inaccuracy is not considered to be a limitation. The excellent agreement over a large range of values for j can be seen in figure 1 (as the large open circles). For purposes of subsequent analyses, however, this 6-term function is cumbersome. Thus, because of the small coefficients for three of the terms (b, d, and e), the expression was further simplified, using just *a, c, and K*, to yield the Good-Smialek approximation (G-S-A):

$$\sum_{i=1}^{j}\sqrt{i}_{GSA} \cong \tfrac{1}{2} j^{1/2} + \tfrac{2}{3} j^{3/2} \qquad [3a]$$

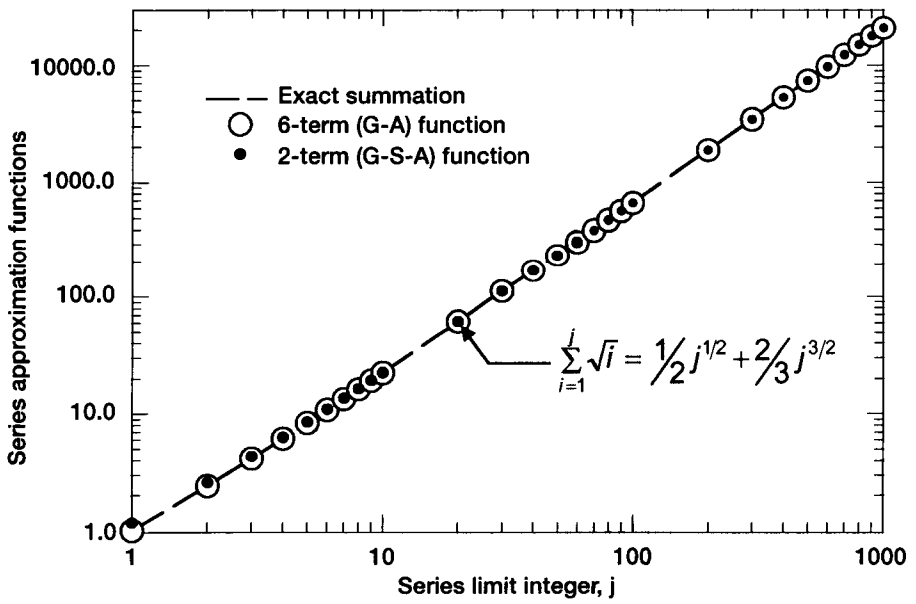

Figure 1.—Comparison of Good-Smialek approximations to $\Sigma\sqrt{i}$.

TABLE 1.—APPROXIMATIONS OF THE FUNCTION $\sum_{i=1}^{j}\sqrt{i}$ FOR A RANGE OF j; COMPARISON TO EXACT VALUE AND RELATIVE ERROR

j	$\sum_{1}^{j}\sqrt{i}$	Eq. 2 G-A	Eq. 3 G-S-A	% error G-A	% error G-S-A
1	1.00000	0.98777	1.16667	-1.222609	16.666667
2	2.41421	2.41061	2.59272	-0.149268	7.394180
3	4.14626	4.14576	4.33013	-0.012123	4.434417
4	6.14626	6.14721	6.33333	0.015414	3.043621
5	8.38233	8.38403	8.57159	0.020210	2.257863
6	10.83182	10.83391	11.02270	0.019250	1.762231
7	13.47757	13.47985	13.66972	0.016899	1.425640
8	16.30600	16.30835	16.49916	0.014424	1.184580
9	19.30600	19.30835	19.50000	0.012190	1.004866
10	22.46828	22.47059	22.66299	0.010275	0.866607
20	61.66598	61.66724	61.86455	0.002054	0.322008
30	112.08285	112.08330	112.28312	0.000402	0.178688
40	171.61579	171.61580	171.81709	0.000005	0.117296
50	239.03580	239.03564	239.23779	-0.000066	0.084504
60	313.50914	313.50902	313.71165	-0.000040	0.064594
70	394.42174	394.42180	394.62465	0.000015	0.051444
80	481.29674	481.29710	481.49997	0.000075	0.042225
90	573.74990	573.75066	573.95340	0.000132	0.035467
100	671.46295	671.46419	671.66667	0.000185	0.030340
200	1892.48421	1892.49430	1892.68915	0.000533	0.010829
300	3472.55639	3472.58364	3472.76187	0.000785	0.005917
400	5343.12753	5343.18273	5343.33333	0.001033	0.003852
500	7464.53424	7464.63030	7464.74026	0.001287	0.002760
600	9810.00023	9810.15175	9810.20642	0.001545	0.002102
700	12359.86190	12360.08479	12360.06821	0.001803	0.001669
800	15098.88039	15099.19165	15099.08680	0.002061	0.001367
900	18014.79350	18015.21100	18015.00000	0.002318	0.001146
1000	21097.45589	21097.99823	21097.66246	0.002571	0.000979

Now the error is $16^2/_3$ % at j = 1, primarily due to ignoring the term K. But, as shown in table 1, this error is quickly reduced to < 1% for j < 10, and to < 0.1% for j > 50. At j = 1000 the error is only 0.001%. This decreasing trend in error is shown in figure 2, where the deviation from the exact solution is only noticeable for j =1 or 2 (small filled circles). Thus, for a reasonably high number of cycles corresponding to most cyclic tests, the simple expression in eq. [3a] provides an excellent approximation.

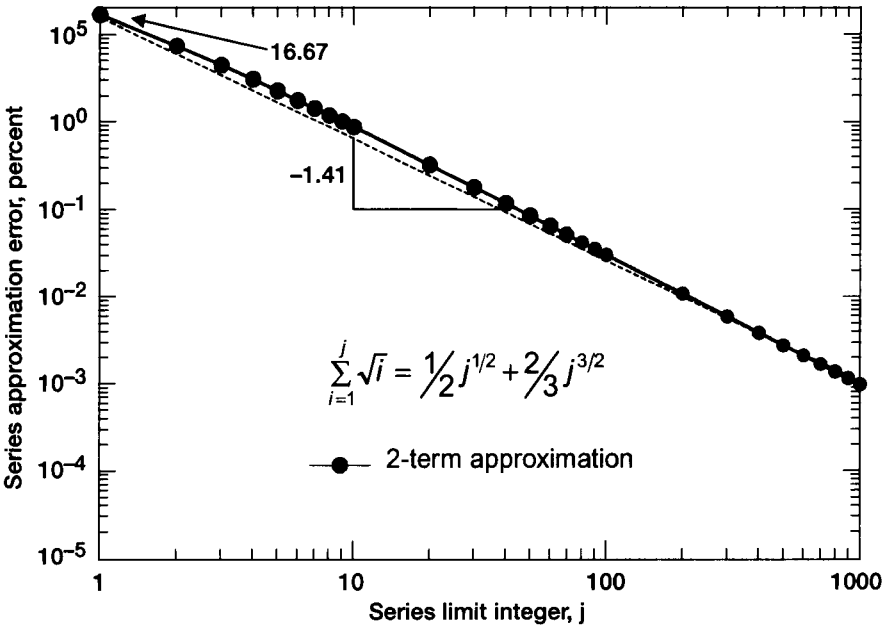

Figure 2.—Relative error (percent) in Good-Smialek approximations relative to $\Sigma\sqrt{i}$.

Considering the nearly linear dependence of error with j in figure 2, a modified and very precise 3-term approximation may be obtained by (GSA'), where –1.41 is the log-log slope of the error versus j plot, and 0.1667 is the fractional error at j = 1:

$$\sum_{i=1}^{j}\sqrt{i}_{\,GSA'} \cong \tfrac{1}{2}j^{1/2} + \tfrac{2}{3}j^{3/2} - \tfrac{1}{6}j^{-1.410} \qquad [3b]$$

Substitution of eq. [3a] into the relations for ΔW/A, eq.'s. [1a,b] and all the other output equations (table 3, Part 1) [1], yields a new set of output equations based on the Good-Smialek Approximation (GSA), where A and B refer to the portions of the curve where $j \le n_o$ and $j \ge n_o$:

$$\left(\frac{\Delta W}{A}\right)_{GSA.A} \cong F_A\sqrt{k_p\Delta t}\left\{\tfrac{1}{2}(2n_o - S_c)(j)^{1/2} + \tfrac{1}{3}(1-2S_c)(j)^{3/2}\right\} \qquad [4a]$$

$$\left(\frac{\Delta W}{A}\right)_{GSA.B} \cong F_A\sqrt{k_p\Delta t}\left\{\left((1-S_c)\,j - \tfrac{1}{2}S_c\right)(n_o)^{1/2} + \tfrac{1}{3}(1+S_c)(n_o)^{3/2}\right\} \qquad [4b]$$

The power of these new expressions is that the weight change and all the other model outputs can be easily and directly calculated for any particular cycle(s) and any desired combination of the model parameters (k_p, Δt, F_A, $[n_o]$, S_c,), as listed in table 2. No iterative calculations requiring a programmed solution are required.

TABLE 2.— LIST OF RELATIONS DESCRIBING VARIOUS OTHER DICOSM MODEL OUTPUTS USING THE GOOD-SMIALEK APPROXIMATION.

Cumulative total weight of oxygen or metal reacted:

$$\Sigma W_{oxy,A}^{GSA} = F_A\sqrt{k_p\Delta t}\left\{n_o\, j^{1/2} + \tfrac{1}{3}\, j^{3/2}\right\}$$

$$\Sigma W_{oxy,B}^{GSA} = F_A\sqrt{k_p\Delta t}\left\{j\, n_o^{1/2} + \tfrac{1}{3} n_o^{3/2}\right\}$$

$$\Sigma W_{met}^{GSA} = (S_c - 1)\,\Sigma W_{oxy}^{GSA}$$

Weight of retained scale, before (W_r') and after (W_r) spallation:

$$W_{r,A}^{'GSA} = S_c F_A\sqrt{k_p\Delta t}\left\{\left(n_o + \tfrac{1}{2}\right) j^{1/2} - \tfrac{1}{3}\, j^{3/2}\right\}$$

$$W_{r,A}^{GSA} = S_c F_A\sqrt{k_p\Delta t}\left\{\left(n_o - \tfrac{1}{2}\right) j^{1/2} - \tfrac{1}{3}\, j^{3/2}\right\}$$

$$W_{r,B}^{'GSA} = S_c F_A\sqrt{k_p\Delta t}\left\{\tfrac{1}{2}\, n_o^{1/2} + \tfrac{2}{3}\, n_o^{3/2}\right\}$$

$$W_{r,B}^{GSA} = S_c F_A\sqrt{k_p\Delta t}\left\{-\tfrac{1}{2}\, n_o^{1/2} + \tfrac{2}{3}\, n_o^{3/2}\right\}$$

Cumulative total weight of oxide spalled (ΣW_s) after j cycles;
Fractional weight of oxide spalled (F_s) on cycle j:

$$\Sigma W_{s,A}^{GSA} = S_c F_A\sqrt{k_p\Delta t}\left\{\tfrac{1}{2}\, j^{1/2} + \tfrac{2}{3}\, j^{3/2}\right\}$$

$$\Sigma W_{s,B}^{GSA} = S_c F_A\sqrt{k_p\Delta t}\left\{\left(j + \tfrac{1}{2}\right) n_o^{1/2} - \tfrac{1}{3} n_o^{3/2}\right\}$$

$$F_{s,A} = \frac{1}{\tfrac{1}{2} + n_o - \tfrac{1}{3} j}$$

$$F_{s,B} = \frac{1}{\tfrac{1}{2} + \tfrac{2}{3} n_o}$$

Equivalent spall constant from COSP model for $j > n_o$.

$$Q_o = \left\{S_c\sqrt{F_A k_p\Delta t}\left(\tfrac{1}{2} + \tfrac{2}{3}\, n_o\right)^2\right\}$$

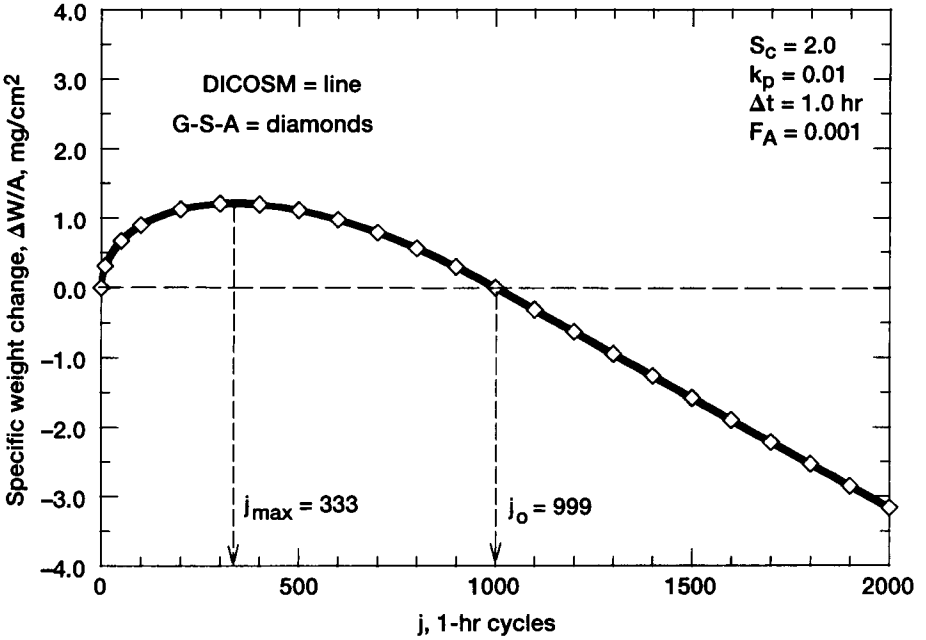

Figure 3.—Comparison of baseline cyclic oxidation weight change curve for exact DICOSM (line) and GSA (symbols) calculations. (S_c = 2.0, k_p = 0.01 mg^2/cm^4 hr, F_A = 0.001, Δt = 1.0 hr).

An example of a DICOSM model cyclic oxidation curve (line), obtained from the full summation series in eq. 1, is shown in figure 3 for the same baseline input parameters utilized in Part 1. Also shown are the results of the GSA calculations (symbols) for the same model case, utilizing eq. 4. Note that there is virtually no distinction under these conditions, and the GSA solution provides a wholly acceptable reproduction of the exact model. The numerical data for these two models are listed in the first two columns of table 3, and there is complete agreement to four decimal places. In fact, it is only in the extreme model cases that any differential can be discerned. Such an example is shown in the last three columns of table 3 for the high values of S_c = 5 and F_A = 0.1. Now appreciable relative errors have been produced in the first few cycles, but here the absolute values of the weight change are quite small. Also, these errors still diminish to less than 1 percent at just 10 cycles. Finally, these high spall fractions and high values of the stoichiometric constant are not characteristic of oxidation resistant materials. In conclusion, the GSA solution to the DICOSM spalling model provides a mathematically robust substitution in most cases, and the more precise GA and GSA' solutions (eq.'s 2 and 3b) are not required.

The various descriptive parameters that define the typical characteristics of a cyclic oxidation curve may now be determined analytically, such as the maximum in weight gain, the time to reach maximum weight gain, the time to cross zero weight change, and the final rate of weight loss. The time to maximum gain is determined by differentiating $(\Delta W/A)_A$ with respect to j in [4a], setting dW/dj equal to zero, and solving for j_{max}. The maximum gain is determined by substituting j_{max} back into equation [4A] for weight change. Finally the time to cross zero weight change is determined by setting $(\Delta W/A)_A$ equal to zero and solving for j_o. Note that because only eq. 4a was used in these derivations, eq.'s. 5-7a, apply only to Case A, $j < n_o$.

TABLE 3.—SPECIFIC WEIGHT CHANGE TABLE (mg/cm^2) OBTAINED FROM THE GSA SOLUTION (eq. 3) COMPARED TO THOSE FROM THE EXACT DICOSM SUMMATION SERIES (eq. 1) FOR TWO EXTREME CASES OF THE CYCLIC OXIDATION SPALLING MODEL

Percent relative error listed for Case 2; zero error for Case 1.

	Sc=2.0 kp=0.01 dt=1 Fa=0.001	Sc=2.0 kp=0.01 dt=1 Fa=0.001	Sc=5.0 kp=0.01 dt=1 Fa=0.100	Sc=5.0 kp=0.01 dt=1 Fa=0.100	Sc=5.0 kp=0.01 dt=1 Fa=0.100
Cycle, j	**1:DICOSM**	**1:GSA**	**2:DICOSM**	**2:GSA**	**% error**
0	0.0000	0.0000	0.0000	0.0000	0.0000
1	0.0998	0.0998	0.0500	0.0450	-10.0000
2	0.1410	0.1410	0.0266	0.0212	-20.3008
3	0.1725	0.1725	-0.0205	-0.0260	26.8293
4	0.1990	0.1990	-0.0844	-0.0900	6.6351
5	0.2223	0.2223	-0.1620	-0.1677	3.5185
6	0.2432	0.2432	-0.2515	-0.2572	2.2664
7	0.2625	0.2625	-0.3514	-0.3572	1.6505
8	0.2803	0.2803	-0.4609	-0.4667	1.2584
9	0.2970	0.2970	-0.5792	-0.5850	1.0014
10	0.3127	0.3127	-0.7057	-0.7115	0.8219
20	0.4378	0.4378	-1.9706	-1.9764	0.2943
30	0.5307	0.5307	-3.2355	-3.2413	0.1793
40	0.6065	0.6065	-4.5004	-4.5062	0.1289
50	0.6710	0.6710	-5.7653	-5.7712	0.1023
60	0.7273	0.7273	-7.0302	-7.0361	0.0839
70	0.7773	0.7773	-8.2951	-8.3010	0.0711
80	0.8220	0.8220	-9.5600	-9.5659	0.0617
90	0.8624	0.8624	-10.8250	-10.8308	0.0536
100	0.8990	0.8990	-12.0899	-12.0957	0.0480
200	1.1300	1.1300	-24.7390	-24.7448	0.0234
300	1.2107	1.2107	-37.3881	-37.3939	0.0155
400	1.1980	1.1980	-50.0372	-50.0430	0.0116
500	1.1158	1.1158	-62.6863	-62.6922	0.0094
600	0.9773	0.9773	-75.3354	-75.3413	0.0078
700	0.7911	0.7911	-87.9845	-87.9904	0.0067
800	0.5629	0.5629	-100.6336	-100.6395	0.0059
900	0.2970	0.2970	-113.2828	-113.2886	0.0051
1000	-0.0032	-0.0032	-125.9319	-125.9377	0.0046
1100	-0.3194	-0.3194	-138.5810	-138.5868	0.0042
1200	-0.6356	-0.6356	-151.2301	-151.2359	0.0038
1300	-0.9518	-0.9518	-163.8792	-163.8850	0.0035
1400	-1.2681	-1.2681	-176.5283	-176.5342	0.0033
1500	-1.5843	-1.5843	-189.1774	-189.1833	0.0031

$$\left(\frac{\Delta W}{A}\right)_{GSA,\max} \cong \frac{F_A\sqrt{k_p\Delta t}}{3}\left\{\frac{(2n_o - S_c)^{3/2}}{(2(2S_c-1))^{1/2}}\right\} \quad [5]$$

$$j_{\max} \cong \frac{2n_o - S_c}{2(2S_c-1)} \quad [6]$$

$$j_{o,A} \cong \frac{3(2n_o - S_c)}{2(2S_c-1)} \quad [7a]$$

$$j_{o,B} \cong \frac{2(S_c+1)n_o - 3S_c}{6(S_c-1)} \quad [7b]$$

It can be seen that the first three relations contain some function of the term $(2n_o\text{-}S_c)/(2S_c\text{-}1)$. Thus the ratio of j_o/j_{max} produces a simple integer, exactly equal to 3.0, the ratio produced by the numerical model and close to those produced (3.3, 3.3, and 3.4) for Al_2O_3 scales by three previous models [2, 3, 5].

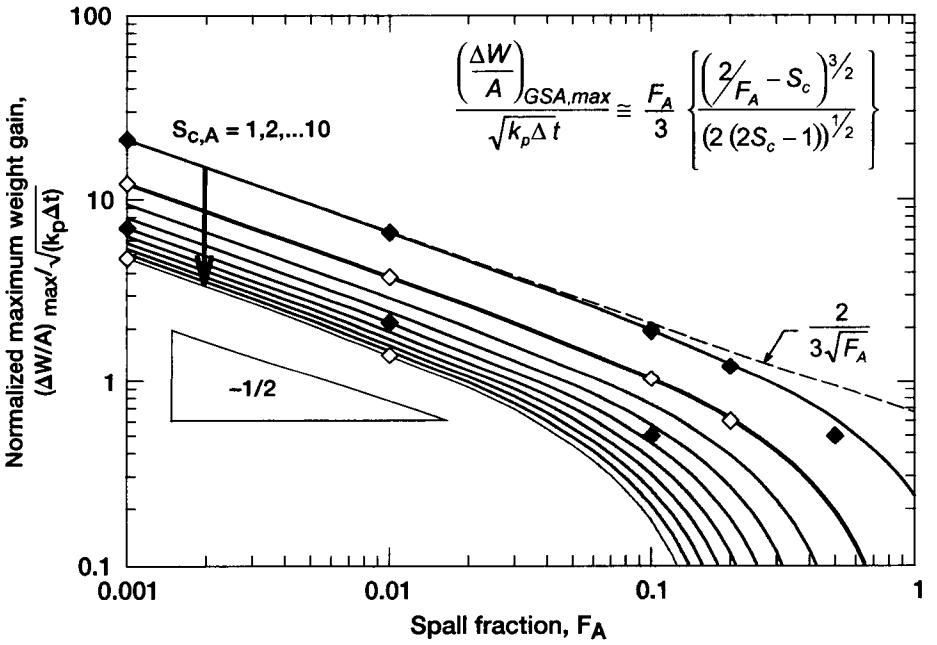

Figure 4.—The effect of spall area fraction, F_A, on the normalized maximum weight change, $(\Delta W/A)_{max}/\sqrt{(k_p\Delta t)}$, according to the GSA solution for the DICOSM model. Lines refer to GSA solution, symbols refer to actual DICOSM calculations).

The dependence of the maximum in the weight change curve $(\Delta W/A)_{max}$ with the spall constant F_A (eq. 5) is shown in figure 4. This family of curves corresponds to the range of all possible values of S_c for the available oxides [1]. (Here $(\Delta W/A)_{max}$ is normalized by the term $(k_p\Delta t)^{1/2}$ to collapse the results for all values of the growth product onto one curve). The case for $S_c = 2.0$ is

shown as the bold curve. It is seen that $(\Delta W/A)_{max}$ varies nearly as $(F_A)^{-1/2}$ for $F_A \leq 0.1$, i.e., for most typical values. This dependency is also evident from inspection of eq. 5, where it is recalled that n_o is defined as $1/F_A$. The effect of increasing S_c is to decrease the level of the maximum weight gain. The values obtained from a few DICOSM model calculations (eq. 1) are shown as symbols and the agreement is excellent for $F_A \leq 0.1$.

The effect of the stoichiometric constant S_c and the spalling constant F_A on the dependence of the number of cycles to reach maximum weight j_{max} (eq. 6) is shown in figure 5. No attempt was made to interpolate a maximum less than one cycle ($j_{max} < 1$). For $F_A \leq 0.1$, j_{max} varies essentially as F_A^{-1}. Good agreement is again found with the DICOSM calculations (symbols). The case for $S_c = 2.0$ is shown as the bold curve. The effect of increasing S_c is to decrease the number of cycles to maximum weight gain. As an extreme example, increasing S_c by a factor of 10, from its theoretical limits of 1 to 10, has the effect of decreasing j_{max} by nearly a factor of 20.

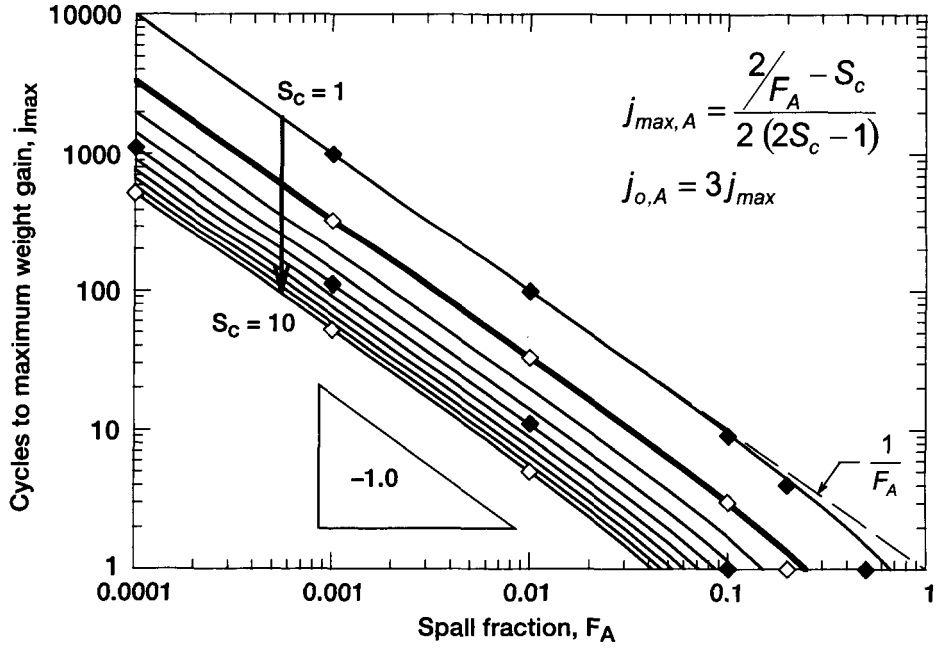

Figure 5.—The effect of spall area fraction, F_A, on the number of cycles, j_{max}, to reach maximum weight change according to the GSA solution for the DICOSM model. Lines refer to GSA solution, symbols refer to actual DICOSM calculations).

The same trends are found for the number of cycles to reach zero weight change, j_o, in figure 6. The case for $S_c = 2.0$ is again shown as the bold curve. While generally similar to the family of curves for j_{max}, there is one difference that could affect the ratio of j_o / j_{max} and the overall shape of the cyclic oxidation curve. This occurs for the exceptions when Case B applies ($j > n_o$) **before** $\Delta W/A$ reached zero weight change. The criterion for this exception is found by setting $j_{o,B} > n_o$ in eq. 7b (Case B), yielding $S_c \leq 8n_o/(4n_o+3)$. This means that S_c must be less than a value very nearly equal to 2.0 (e.g., 1.860, 1.985, or 1.999 for $n_o = 10$, 100, or 1000, respectively).

Alternately stated, eq. 7a (Case A) or eq. 7b (Case B) must be used to obtain j_o depending on whether $S_c \geq 2$ or $S_c \leq 2$, respectively. Thus two sets of curves are presented for j_o in figure 6, corresponding to Case A (lower) and Case B (upper). In terms of the cyclic oxidation weight

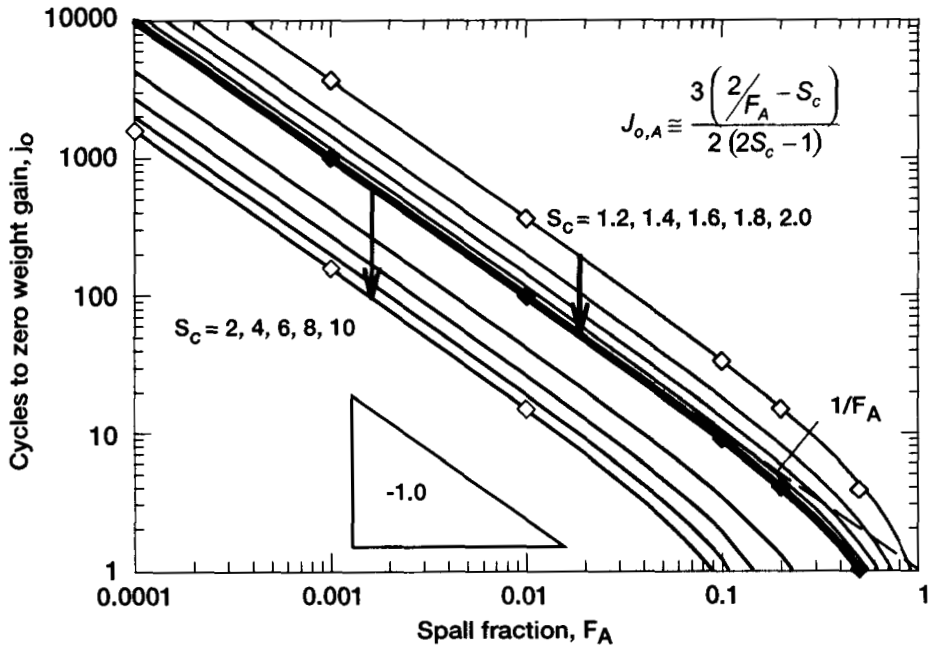

Figure 6.—The effect of spall area fraction, F_A, on the number of cycles, j_o, to reach zero weight change, according to the GSA solution for the DICOSM model. (Lines refer to GSA solution, symbols refer to actual DICOSM calculations).

change curve, this means that a linear terminal slope is reached before zero weight change occurs ($S_c \leq 2$, Case B). This special case would therefore occur only for SiO_2 (1.878), Li_2O (1.868), BeO (1.563), and B_2O_3 (1.450) [1]. The simple ratio of $j_o/j_{max} = 3$ no longer applies because eq. 7a no longer applies. In the extreme, for the limiting but impossible case where $S_c = 1$, the final slope is zero, the curve is horizontal, and zero weight change is never achieved.

In this regard, the slope of the latter portion of the curve can always be described by:

$$T.S. = -(S_c - 1)\, F_A \sqrt{n_o k_p \Delta t} \qquad [8]$$

where T.S. is the terminal slope of the cyclic oxidation weight change curve. This relationship is obtained by differentiating the DICOSM model eq. 1b or the GSA model eq. 4b with respect to j. From the definition that $F_A = 1/n_o$, eq. 8 can be restated as:

$$T.S. = -(S_c - 1)\sqrt{F_A k_p \Delta t} \qquad [9]$$

It is therefore apparent that the severity of the final slope increases with S_c, $F_A^{1/2}$, $k_p^{1/2}$, and $(\Delta t)^{1/2}$ and is thus affected by the oxide type as well as by the growth and spalling parameters.

The fractional amount of scale spalled each cycle also reaches a constant value for each cycle. It can be seen from figure 4 and table 1 of Part 1 to be given by [1]:

$$F_{s,B} = \frac{\sqrt{n_o}}{\sum_{i=1}^{n_o} \sqrt{i}} \qquad [10]$$

This can be simplified by using the GSA solution for the summation series to:

$$F_{s,B} = \left(1/2 + 2/3\, n_o \right)^{-1} \cong 3/2\, F_A \qquad [11]$$

That is to say that the scale mass fraction spalled per cycle approaches 1.5 times the area fraction spalled.

2.2 Universal cyclic oxidation curve.

The simplicity of the various descriptive parameters presented in eq.'s. [5-11] suggest that a universal function may be developed to describe cyclic oxidation for any set of input parameters. Such a curve should show all the pertinent features of the model curves, but be normalized by characteristic weight and cycle factors. This single curve, in dimensionless parameters, would represent the general behavior produced by any combination of model parameters. By inspection of eq.'s. 4-6, the maximum weight gain, $(\Delta W/A)_{max}$, and the cycle time to reach this maximum, j_{max}, were selected as these characteristic factors. The normalized weight change and cycle number in equation [4a] gives the following relationship for Case A, $j \leq n_o$:

$$W_u = 1/2 \left[3 J_u^{1/2} - J_u^{3/2} \right] \qquad [12]$$

where W_u is the normalized weight change and J_u is the normalized cycle number. The results of such a plot are shown as the dashed master curve in figure 7. Thus, for any value of S_c (≥ 2), F_A, k_p, or Δt, the same universal curve is obtained from eq. [12] for Case A (when $j \leq n_o$).

This is an extremely brief and concise equation defining the initial branch of the cyclic oxidation curve, with simply defined features. At the maximum in weight change, $dW_u/dJ_u = 0$, both $J_{u,max} = 1.0$ and $W_{u,max} = 1.0$. Also, at the cross over point of zero weight change, $W_{u,0} = 0.0$ and $J_{u,0} = 3.0$.

For Case B, starting at the point where $j = n_o$, the secondary branches of the curve require eq. [4b]. In terms of the universal curve, this point is given by $J_u = n_o/j_{max}$, where j_{max} is given by eq. [6]. A listing of these critical points and the slopes of the subsequent linear portions of the universal curve are listed in table 4. It is seen that $J_{u,B}$ is approximately equal to $(2S_c\text{-}1)$ for reasonably large values of $n_o \geq 100$ ($F_A \leq 0.01$). (For $S_c = 2.0$ (near Al_2O_3), the effect of n_o is minimal). For increasing stoichiometric factors, these secondary branches depart from the universal curve at larger values of J_u with increasingly negative slopes and with more sensitivity to low n_o. The limiting values of these critical points are shown as the diamond symbols in figure 7.

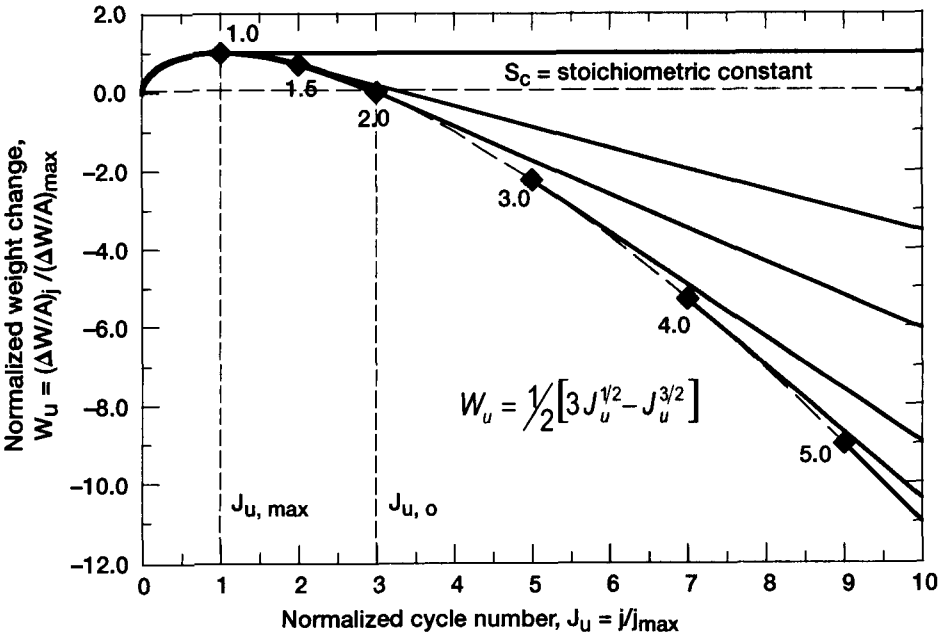

Figure 7.—Semi-universal cyclic oxidation curves for all DICOSM model cases, i.e., normalized weight change (W_u) and normalized cycle numbers (J_u) as derived from GSA solution. One master curve is obtained with linear weight loss rate branches produced at different J_u and with different slopes corresponding to different stoichiometric constants, S_c.

As previously presented, the linear-sloped second branches (Case B) commence after these points corresponding to $j = n_o$, and are given by differentiating W_u with respect to J_u (or from eq. 9):

$$\left(\frac{dW_u}{dJ_u}\right)_{GSA,B} = \frac{3(1-S_c)n_o^{1/2}}{[2(2n_o - S_c)(2S_c - 1)]^{1/2}} \qquad [13]$$

The slopes are seen to increase with S_c and n_o in a complex fashion and are listed in table 4. (At $S_c = 2.0$, the effect of n_o is minimal). Composite curves are shown in figure 7 for the cases where S_c is varied from 1.0 to 5.0, which encompass the vast majority of typical oxides. The secondary branches correspond to the limits approached for reasonably large values of $n_o \geq 100$ ($F_A \leq 0.01$), table 4.

For most typical values of S_c (above 2.0), $W_{u,0} = 0$ at $J_{u,0} = 3$, (corresponding to $j = j_0 = 3j_{max}$). Thus the universal cross over point is defined by $J_u = 3$ for most oxides. However, it should be noted that if $S_c < 2$, then $j \geq n_o$ and Case B applies **before** j reaches $3j_{max}$, i.e., before J_u reaches 3. Accordingly, the constant ratio of $j_o/j_{max} = 3$ (defined by eq.'s. 6 and 7a) no longer applies, and eq.'s. 6 and 7b now suggest a variable j_o/j_{max} ratio. For example, the secondary branch of the curve for $S_c = 1.5$ in figure 7 is seen to depart from the universal curve before reaching zero normalized weight, which now must occur at some $J_u > 3.0$.

Yet for a given oxide scale, where S_c is fixed, a single normalized curve may be used to represent the behavior of practically any combination of the input parameters, k_p, Δt, and F_A (n_o).

TABLE 4.—CRITICAL VALUES OF THE NORMALIZED CYCLE NUMBER, J_{u,B^*}, MARKING THE COMMENCEMENT OF THE LINEAR SLOPE BRANCH, $dW_u/dJ_{u,B}$, FOR THE UNIVERSAL CYCLIC OXIDATION CURVE

Effect of stoichiometric constant S_c and n_o.

S_c	$2S_c$-1	J_{u,B^*}	J_{u,B^*}	J_{u,B^*}		$(dW_u/dJ_u)_B$	$(dW_u/dJ_u)_B$	$(dW_u/dJ_u)_B$	$(dW_u/dJ_u)_B$
	limit as $n_o \rightarrow \infty$	n_o = 1000	n_o = 100	n_o = 10		limit as $n_o \rightarrow \infty$ (mg/cm^2)	n_o = 1000 (mg/cm^2)	n_o = 100 (mg/cm^2)	n_o = 10 (mg/cm^2)
1	1.00	1.00	1.01	1.05		0.00	0.00	0.00	0.00
2	3.00	3.00	3.03	3.33		-0.87	-0.87	-0.87	-0.91
3	5.00	5.01	5.08	5.88		-1.34	-1.34	-1.35	-1.46
4	7.00	7.01	7.14	8.75		-1.70	-1.70	-1.72	-1.90
5	9.00	9.02	9.23	12.00		-2.00	-2.00	-2.03	-2.31
6	11.00	11.03	11.34	15.71		-2.26	-2.26	-2.30	-2.70
7	13.00	13.05	13.47	20.00		-2.50	-2.50	-2.54	-3.10
8	15.00	15.06	15.63	25.00		-2.71	-2.72	-2.77	-3.50
9	17.00	17.08	17.80	30.91		-2.91	-2.92	-2.98	-3.92
10	19.00	19.10	20.00	38.00		-3.10	-3.10	-3.18	-4.38

The Good-Smialek approximation of the DICOSM model has allowed for this construction of a simple, semi-universal cyclic oxidation curve, from which the behavior of any well-behaved data set may be assessed.

2.3 Comparison to high temperature alloy behavior.

Ideally, the systems most applicable to the DICOSM model should exhibit primarily parabolic growth, interfacial spallation occurring at a relatively constant area fraction, the absence of any initial transient or transition oxides, and no break away behavior into different scale phases. It has been shown that single crystal superalloys exhibit substantial interfacial spallation modes. However they are not always immune to transient oxidation or changes in scale make-up.

The results for two PWA 1480 coupons are presented in figure 8 [6]. These coupons had been hydrogen annealed (desulfurized) to two sulfur levels, resulting in clearly differentiated cyclic behavior. Both exhibited a rapid initial weight gain. It was determined to be 0.2 mg/cm^2 by back extrapolation to zero time on a $t^{1/2}$ parabolic plot. This transient amount was accordingly subtracted off the entire weight change curve. (This adjustment can be tolerated for fitting the growth kinetics (k_p). However, it is likely to induce small and gradual errors in the weight loss calculations since this transient layer will also be removed as portions of the underlying scale spall.) The modified data in figure 8 was fit with two DICOSM models shown as the solid lines, with good agreement for the 0.14 ppm S sample (20-6) out to 800 hours and for the 0.8 ppm S sample up to 500 hours. It is realistically demonstrated that the latter sample exhibited an order of magnitude increase in the spall area fraction, F_A. A factor of two increase in the parabolic growth rate also appeared necessary for the best fit, possibly due to mechanism (scale chemistry) changes caused by spallation and aluminum depletion.

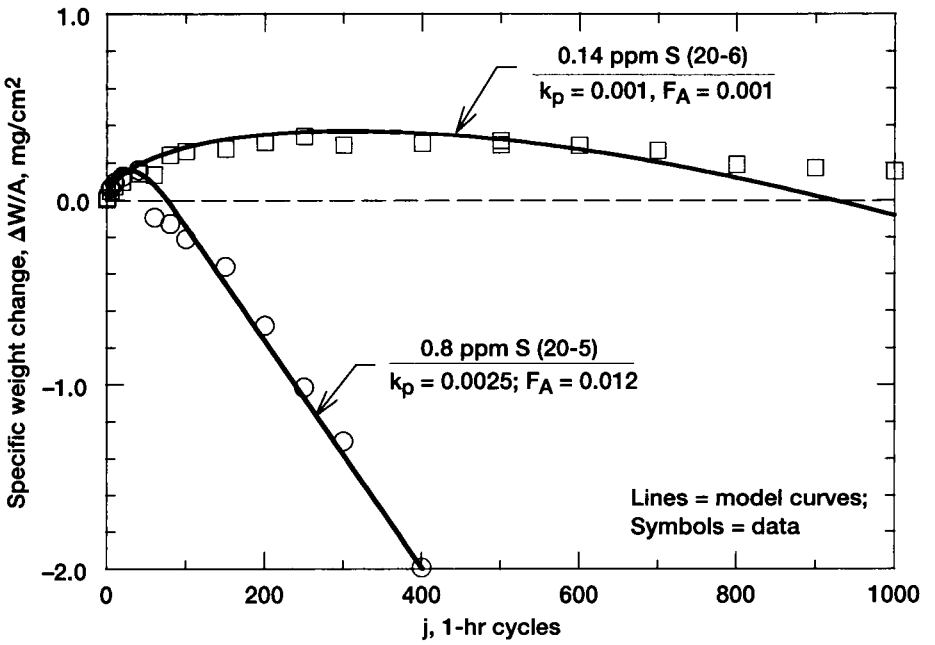

Figure 8.—Comparison of DICOSM model fits (lines) to actual cyclic data (symbols) for two PWA 1480 samples hydrogen annealed to two different sulfur levels. (1100 °C, 1-hr cycles, 0.14 and 0.8 ppmw sulfur).

These curves are plotted according to the universal curve format in figure 9. (Here the data had first been further corrected to eliminate a number of discontinuous drops in weight, due to water immersion testing or extended exposure to humid lab air, in an attempt to produce a more well-behaved cyclic curve. See, for example, ref.'s [6,8]). The corrected data is seen to fall essentially on top of each other for the two curves up until $J = J_o$. There is also good agreement with the normalized model curves up to this point. However, beyond that point, the experimental data for the 0.8 ppm sample appears to diverge negatively from the expected behavior. This is due in part to the difficulty in determining the precise time and amount of the maximum when it occurs early in the cyclic test for a rapidly spalling alloy. This high degree of relative error in defining j_{max} produces a magnified effect on the normalized curve. Another factor is the transition of the scale to heavier oxides, i.e., with larger values of S_c. Indeed, x-ray diffractometer scans had identified a transition from Al_2O_3 (S_c = 2.1243) to $NiTa_2O_6$ (S_c = 5.3813) as the strongest pattern in the last 500 hr of testing. This deviation is consistent with the universal curve for Case A being followed past J = 9 for systems with $S_c \geq 5$, as in figure 7.

A different data set is given in figure 10 for the more adherent scales on NiAl(Zr) oxidized at 1100 and 1200 °C [7]. This data was fit better by the uniform outer layer spallation model (COSP) [2,5], rather than by the interfacial mechanism (DICOSM) [1]. The fitted curves show excellent agreement with the data. Although there is no rigorous mathematical argument for constructing a universal cyclic curve from a COSP model, the similar behavior to DICOSM models suggests a similar plot, figure 11. Here the data and model curves for two different temperatures (k_p's) and two different spall constants (Q_o) are seen to follow a nearly a single universal normalized plot, presumably that corresponding to Al_2O_3 scales. For COSP models, $J_{u,o}$ should ideally be equal to 3.3 for alumina, as suggested by the 1100 °C model prediction. The 1200 °C curve, using j_{max} determined from the data in fig. 10, deviates slightly from this ratio, indicating less than ideal COSP behavior.

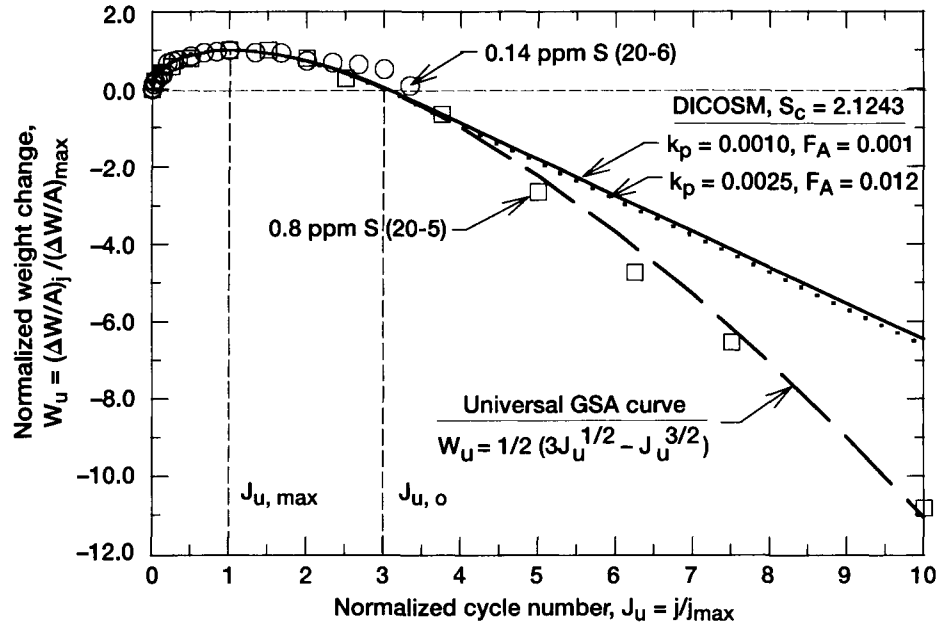

Figure 9.—Universal (normalized) cyclic oxidation curves for two PWA 1480 samples exhibiting different behavior (from Figure 5). (DICOSM model fits (lines); experimental data (symbols)).

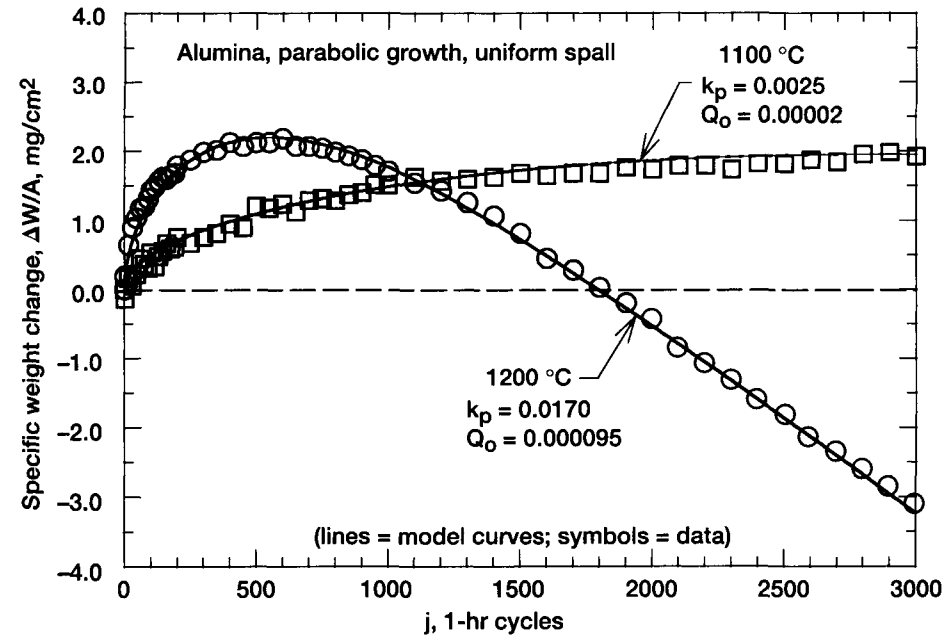

Figure 10.—Comparison of COSP model fits (lines) to actual cyclic data (symbols) for NiAl at 1100 °C and 1200 °C with 1-hr cycles.

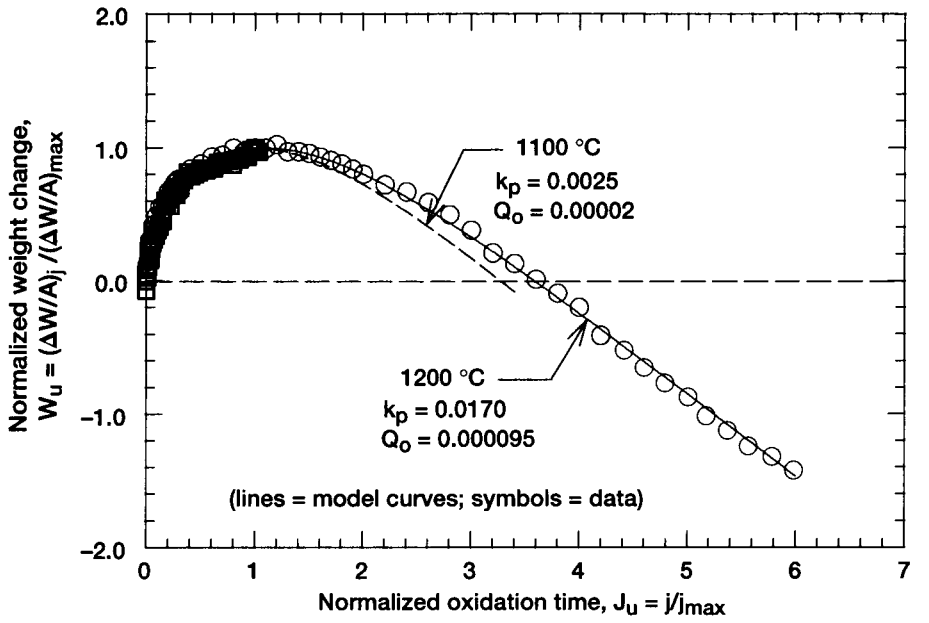

Figure 11.—Universal (normalized) cyclic oxidation curves for NiAl oxidized at 1100 °C and 1200 °C (from Figure 7). (COSP model fits (lines); experimental data (symbols)).

This overall success suggests that a universal cyclic oxidation curve for all COSP model cases may also be produced by a similar construction. While the mathematics of the uniform layer spallation model of COSP does not allow for the direct calculation of such a curve, it is still possible to run a spectrum of different cases and obtain the corresponding values of $(\Delta W/A)_{max}$ and j_{max}. The results of such an exercise, in which model variables were changed using COSP for Windows [5] (k_p from 0.001 to 0.01 mg/cm^{2}hr ; Δt from 0.1 to 10 hr, and Q_o from 0.001 to 0.01), were all shown to produce a single curve for each value of S_c used (i.e., 1, 2, 3, 4, 5), figure 12. The overall behavior parallels that constructed for the DICOSM case presented in figure 7. The universal DICOSM curve for Case A, ($j \leq n_o$, eq. 12), shown as the dashed line, is seen to follow the initial portions of the COSP curves . However the COSP universal plot shows no unique value of the ratio of J_o/J_{max} for all oxides, whereas the DICOSM model sets this ratio as 3.0 for all $S_c \geq 2$. Furthermore, the linear portions of the curves begin earlier and are more shallow than their DICOSM model counterparts (i.e., corresponding to the same values of S_c).

It is therefore proposed that these constructions may be used for long term projections of incomplete cyclic curves or to compare the ideality and scale stoichiometry produced for various alloys under various test conditions. Further shakedowns to discover weaknesses in the construction are needed to more fully define the limitations of the technique.

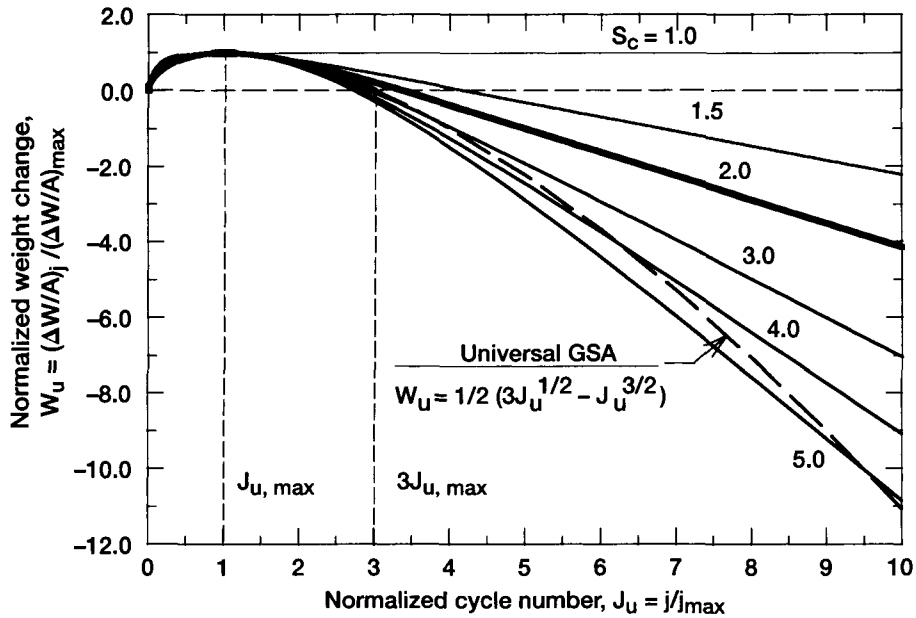

Figure 12.—Universal (normalized) cyclic oxidation curves for all COSP model conditions. Dashed curve corresponds to DICOSM GSA curve, Case A, from Figure 9.

3. Summary

A succinct, simple, and accurate algebraic expression has been developed as an approximation for the summation series of the square root of an integer. Substitution for this series in the DICOSM model of Part 1 has produced the Good-Smialek approximation (GSA), which faithfully and accurately reproduces all the features of the original spalling model. Essentially no error is introduced except for cases exhibiting an extreme amount of spalling, and then for only a small number of initial cycles. Other outputs germane to these models, (the amount of metal consumed, amount of retained oxide, the fraction and total amount of spalled oxide), may also be obtained from similar relationships.

The simplified mathematics has also allowed for the formulation of descriptive parameters as direct functions of the input parameters. Consequently, the maximum weight change, the number of cycles to reach maximum, the number of cycles to reach zero weight change, and the final rate of weight loss may all be calculated directly. These regular dependencies further suggest a uniform behavior for any combination of cyclic oxidation model input parameters. Accordingly a universal cyclic oxidation curve was constructed, simply by normalizing the weight change and cycle number by the maximum in weight change and the number of cycles to reach the maximum, respectively. Universal behavior was found for these normalized curves for all values of the growth constant and cycle duration, and most values of the interfacial area spall fraction. Bifurcations from this curve were obtained only for different values of the stoichiometric constant (chemistry) of the oxide scale. A similar construction was found to apply for the uniform outer layer spallation model (COSP), but with shifts in the position and slope of the final linear loss portions.

Actual cyclic oxidation data for PWA 1480 was analyzed and compared to the DICOSM interfacial spall model with reasonable success. Two different behaviors due to different sulfur contents were described by the universal cyclic oxidation construct. Alternately, data for NiAl(Zr), oxidized at two different temperatures, was successfully modeled by the uniform spall layer model in COSP. These in turn were also successfully normalized as nearly congruent universal cyclic oxidation plots.

References

1. Smialek, J.L., A Deterministic Interfacial Cyclic Oxidation Spalling Model: Part 1.—Model Development and Parametric Response, NASA/TM—2002-211906-Part1.
2. Lowell, C.E., Barrett, C.A., Palmer, R.W., Auping, J.V., Probst, H.B., Oxid. Met., 1991, 36: 81–112.
3. Smialek, J.L., Metall. Trans., 1978, 9A: 309–320.
4. Good, B.S., private communication, NASA Glenn Research Center, 2001.
5. Smialek, J.L., Auping, J.V., Oxid. Met., 2002, 57: 559–581.
6. Smialek, J.L., Toward Optimum Scale and TBC Adhesion on Single Crystal Superalloys in E.J. Opila, P.Y. Hou, D. Shores, M. McNallan, and R. Oltra , eds. High Temperature Corrosion and Materials Chemistry, vol. **98–9.** Pennington, NJ: The Electrochemical Society, 1998. pp 211–220.
7. Barrett, C.A., Oxid. Met., 1988, 30: 361–391.
8. Smialek, J.L., Morscher, G.N., Mater. Sci. Engineer., 2002, A332: 11–24.

REPORT DOCUMENTATION PAGE

Form Approved
OMB No. 0704-0188

1. AGENCY USE ONLY (*Leave blank*)	2. REPORT DATE	3. REPORT TYPE AND DATES COVERED
	December 2002	Technical Memorandum

4. TITLE AND SUBTITLE

A Deterministic Interfacial Cyclic Oxidation Spalling Model: Part 2.—Algebraic Approximation, Descriptive Parameters, and Normalized Universal Curve

5. FUNDING NUMBERS

WBS–22–708–73–05

6. AUTHOR(S)

James L. Smialek

7. PERFORMING ORGANIZATION NAME(S) AND ADDRESS(ES)

National Aeronautics and Space Administration
John H. Glenn Research Center at Lewis Field
Cleveland, Ohio 44135–3191

8. PERFORMING ORGANIZATION REPORT NUMBER

E–13596–2

9. SPONSORING/MONITORING AGENCY NAME(S) AND ADDRESS(ES)

National Aeronautics and Space Administration
Washington, DC 20546–0001

10. SPONSORING/MONITORING AGENCY REPORT NUMBER

NASA TM—2002-211906-PART2

11. SUPPLEMENTARY NOTES

Responsible person, James L. Smialek, organization code 5160, 216–433–5500.

12a. DISTRIBUTION/AVAILABILITY STATEMENT

Unclassified - Unlimited
Subject Category: 26 Distribution: Nonstandard

Available electronically at http://gltrs.grc.nasa.gov

This publication is available from the NASA Center for AeroSpace Information, 301–621–0390.

12b. DISTRIBUTION CODE

13. ABSTRACT ***(Maximum 200 words)***

A cyclic oxidation interfacial spalling model has been developed in Part 1. The governing equations have been simplified here by substituting a new algebraic expression for the series $\Sigma\sqrt{i}$ (Good-Smialek approximation). This produced a direct relationship between cyclic oxidation weight change and model input parameters. It also allowed for the mathematical derivation of various descriptive parameters as a function of the inputs. It is shown that the maximum in weight change varies directly with the parabolic rate constant and cycle duration and inversely with the spall fraction, all to the 1/2 power. The number of cycles to reach maximum and zero weight change vary inversely with the spall fraction, and the ratio of these cycles is exactly 1:3 for most oxides. By suitably normalizing the weight change and cycle number, it is shown that all cyclic oxidation weight change model curves can be represented by one universal expression for a given oxide scale.

14. SUBJECT TERMS

High temperature; Oxidation; Metals; Spalling; Computer programs; Thermal cycling; Modeling; Kinetics; Nickel alloys

15. NUMBER OF PAGES

25

16. PRICE CODE

17. SECURITY CLASSIFICATION OF REPORT	18. SECURITY CLASSIFICATION OF THIS PAGE	19. SECURITY CLASSIFICATION OF ABSTRACT	20. LIMITATION OF ABSTRACT
Unclassified	Unclassified	Unclassified	